

# In-depth micro-spectrochemical analysis of archaeological Egyptian pottery shards

A. Khedr · M.A. Harith

Received: 12 April 2013 / Accepted: 18 June 2013 / Published online: 14 July 2013  
© Springer-Verlag Berlin Heidelberg 2013

**Abstract** Old Egyptian pottery samples have been in-depth microchemically analyzed using laser induced breakdown spectroscopy (LIBS), energy dispersive X-ray (EDX), and X-ray diffraction (XRD) techniques. Samples from two different ancient Islamic eras, Mamluk (1250–1517 AD), Fatimid (969–1169 AD) in addition to samples from the Roman period (30 BC–395 AD) were investigated. LIBS provided the analytical data necessary to study in micrometric steps the depth profiling of various elements in each sample. Common elements such as silicon, calcium, and aluminum relevant to the originally manufactured and processed clay, showed up in all the investigated samples. EDX and XRD techniques that have been used in the present work provided important chemical insight about the structure of the samples. The obtained analytical results demonstrated the possibility of using LIBS technique in performing in situ spectrochemical analysis of archaeological pottery. This leads to fast in-depth spatial characterization of the samples in the micron range with nearly invisible surface destructive effects. There is no doubt that this can help in restoration and conservation of such precious objects.

## 1 Introduction

Analytical techniques are vital to artworks conservation and restoration since they provide substantial information regarding the physical and chemical structure of such precious objects. In addition, analysis of an artwork elucidates the importance of the chemical components included

and characterizes its preservation state in view of external parameters effects. This extends to different conservation studies, from identification of substrate and top layer materials through mapping of the compositional structure and careful removal of unwanted layers (encrustation, overpainting, old varnish, etc.) [1]. Therefore, many powerful analytical methods developed as a result of the technological progress in optoelectronics are adopted to solve different and complex problems, arising in art conservation [2–4]. Optical Microscopy (OM), Scanning Electron Microscopy (SEM), SEM and Energy Dispersive X-Ray analysis (SEM-EDX) [5–8], X-Ray Diffraction (XRD) [9–11], X-Ray Fluorescence (XRF) [12], and Proton Induced X-ray Emission Spectrometry (PIXE) [13] are important examples of such analytical techniques.

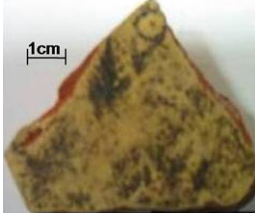
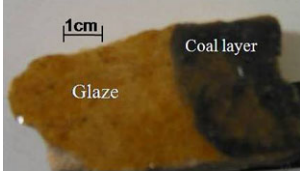

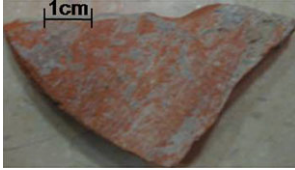
However, laser-based analytical techniques have the advantage over conventional techniques by being nondestructive, need no sampling, of high sensitivity and selectivity, possibly portable, short measurement time, provide spatial and microscopic resolution as well as depth profiling and multielemental analysis. These characteristic advantages are inherent of techniques such as laser Raman spectroscopy, and laser induced fluorescence (LIF). However, the search for alternative analytical methods, which can be used outdoor with moderate expenses and efforts led us to consider the analytical potential of laser induced breakdown spectroscopy (LIBS).

LIBS has been extensively used in the cultural heritage field as an advanced tool in the elemental analysis and characterization of the ancient cultural objects. Some examples of such archeological samples that have been characterized by LIBS include metals, ceramics, paints, rocks, marble, bone, and manuscripts [14–21]. An outstanding application of LIBS occurs in the study of pottery samples with multi-layer decorated surfaces, glazes or surface coatings [22–24],

---

A. Khedr · M.A. Harith (✉)  
National Institute of Laser Enhanced Science, Cairo University,  
Cairo, Egypt  
e-mail: mharithm@niles.edu.eg  
Fax: +20-2-35675335

**Table 1** Photos and specifications of the studied pottery shards

Identification	Shards photos	Source
<p><i>Glaze upperlayer shards</i></p> <p><b>S1:</b> ceramic with contaminated crust of 100 <math>\mu\text{m}</math> thickness.</p>		Mamluk (1250–1517AD), glazed ceramic collected from Al-Fustat-Cairo excavation store.
<p><b>S2:</b> Ceramic with artificial crust of coal of 160 <math>\mu\text{m}</math> thickness.</p>		Glazed ceramic refer to Fatimid period (969–1169AD), and collected from Al-Fustat excavation store in Cairo.
<p><i>Shards without glaze</i></p> <p><b>S3:</b> Pottery with contaminated white crust of 200–500 <math>\mu\text{m}</math> thickness.</p>		Sample collected from Excavation at Shekho Mosque at Al Saliba street-old Cairo and refers to Mamluk period (1250–1517AD), the mosque was built on 1350 AD.
<p><b>S4:</b> Pottery with contaminated crust of 180 <math>\mu\text{m}</math> thickness.</p>		Sample was collected from Ehnasia el-Medina (12th dynasty) about 120 km from Cairo and refers to late roman period (30 BC–395 AD).

in particular when efforts are addressed to obtain compositional depth profiles of the ceramic samples to distinguish different layers, few tens of micrometers thick [25].

Pottery always reflects contemporary tastes so it is an ideal subject of art-historical study. Different shapes and decorations were used at different times, by different people, and for different purposes. Therefore, by studying pottery, archaeologists can date their sites and say a great deal about ancient cultures. It provides information about technology, craft specialization, trade, industry, art, diet, and a host of other attributes of ancient cultures [26, 27].

In the present work, different Egyptian pottery shards have been selected for analytical characterization adopting LIBS. Table 1 lists the four samples investigated in the present work with their relevant information. One of the selected shards S4 (from the Roman period, 30 BC–395 AD) was covered with hard crust and collected from Ehnasia in Upper Egypt, 120 km south of Cairo. The other samples S1, S2, and S3 are referring to the Islamic period and were collected from El-Fustat excavation store in the vicin-

ity of Cairo. El-Fustat is the name of the first Islamic capital of Egypt, established shortly after the Islamic conquest of Egypt in 641AD. El-Fustat was an important center of ceramic production when Fatimids and Mamluks over took the Islamic Empire. The primary aim of the work presented here is to demonstrate the potentials of LIBS as a fast and simple spectrochemical analytical technique in the classification of old pottery by in-depth microanalysis of the different layers of ceramic shards. In the majority of cases, complementary measurements using energy dispersive X-ray analysis (EDX) and X-Ray diffraction (XRD) studies have been provided.

## 2 Experimental methodology

The experimental setup for LIBS measurements consists of an Nd:YAG laser (BRIO, Quantel, France) operating at its fundamental wavelength  $\lambda = 1064$  nm, pulse duration  $\tau = 5$  ns, energy  $E = 100$  mJ/pulse, and 20 Hz rep-

etition rate. The laser pulse energy used for LIBS analysis was 50 mJ/pulse measured by a Joule meter (SCIEN-TECH, model AC5001, USA energy meter). The laser beam was focused by a planoconvex lens of focal length 100 mm onto the sample surface. The plasma optical emission was collected by a fused-silica optical fiber with a diameter of 600  $\mu\text{m}$  held at a distance of 2 cm above the plasma at an angle of  $30^\circ$  with respect to the target surface. The collected plasma emission is then fed via the other end of the optical fiber to the entrance slit of an echelle spectrometer (Mechelle 7500, Multichannel, Sweden) with a focal length of 17 cm and f-number of 5.2. The spectrometer provides a constant spectral resolution of 7500 corresponding to 4 pixels FWHM, over a wavelength range of 200–1000 nm, displayable in a single spectrum. A gateable ICCD camera (DiCAM-Pro, PCO computer optics, Germany), with a high-resolution sensor with  $1280 \times 1024$  pixels ( $9 \times 9 \text{ mm}^2$ ) coupled to the spectrometer, was used for the detection of the dispersed light. The 25 mm microchannel plate is from DiCAM with a UV-enhanced photocathode. The overall linear dispersion of the Mechelle spectrometer–camera system ranges from 0.0078 (at 200 nm) to  $0.032 \text{ nm pixel}^{-1}$  (at 700 nm). The ICCD camera control was performed via special multichannel instrument software. To avoid electronic interference and jitters, the CCD intensifier high voltage was triggered optically at a typical optimized delay time of 1500 ns and gate width 2000 ns. Such values of delay time and gate width are obtained after a systematic optimization procedure. Emission spectra were recorded for a single laser pulse, and were subsequently analyzed. For depth profiling study, the spectra were collected and analyzed separately for each one of several successive laser pulses. The elemental lines of the emission spectra were identified using LIBS<sup>++</sup> software. The layers thicknesses and craters depth were measured with a calibrated Olympus optical microscope (Spectra services.INC-Rochester NY-BH-2).

Complementary measurements have been performed to identify and quantify the key elements and minerals associated with the ceramic samples using Philips Analytical X-Ray Diffractometer (PW1840, Tube anode Cu, Generator tension 40 kV, and current of 30 mA) and an EDX-system (OXFORD INCA Penta FETx3, England).

### 3 Results and discussion

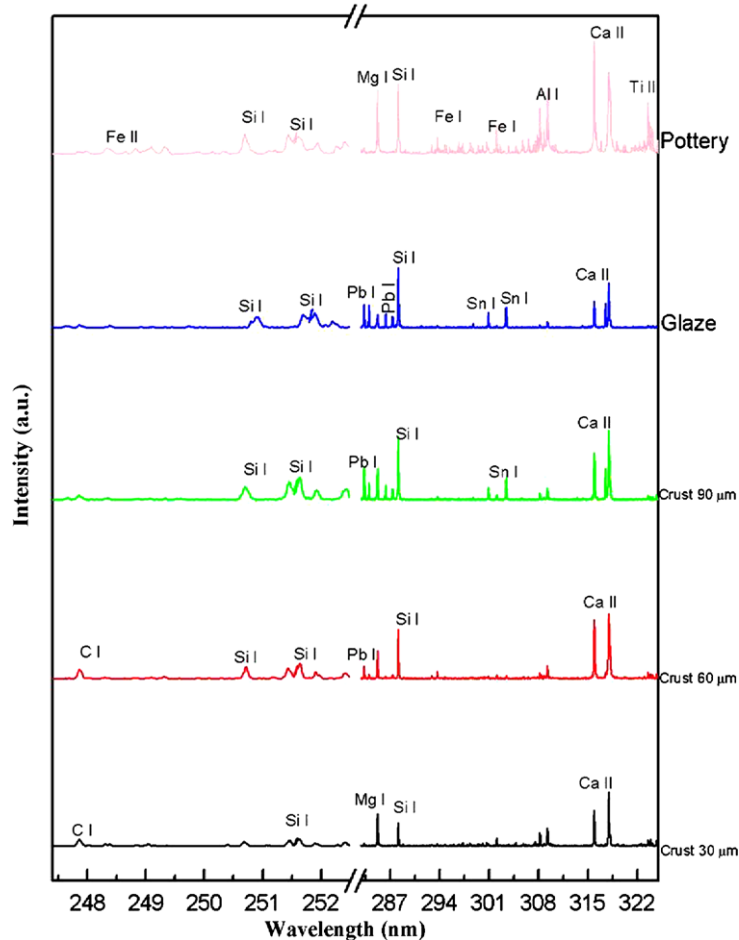
From the historical and artistic point of view, the object's value is a critical factor, which often imposes limitations on the analysis. The approach for analyzing valuable objects can be very different from that used in examining pottery shards from an archeological excavation.

#### 3.1 LIBS analysis

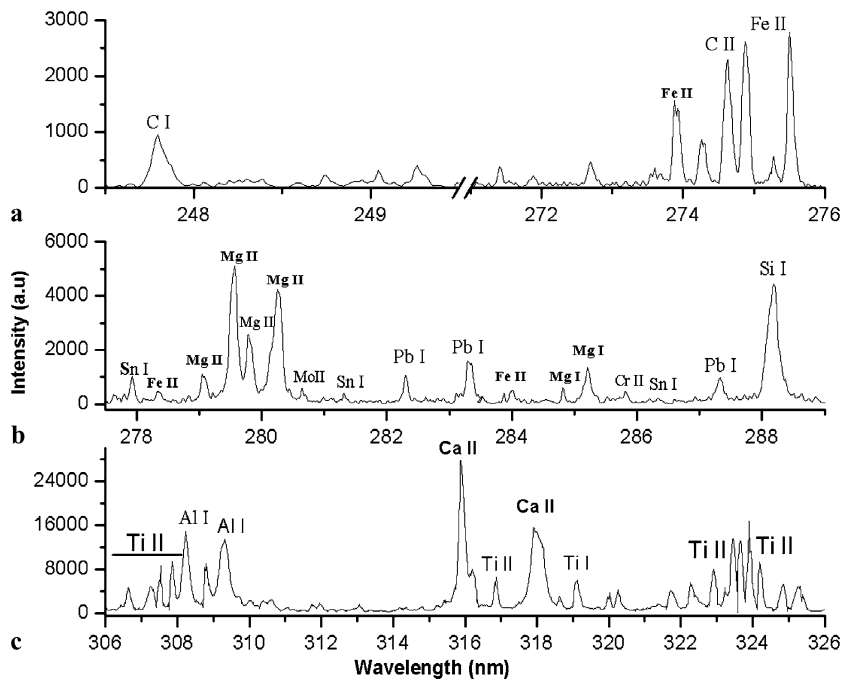
In this context, LIBS is, in principle, a straightforward elemental analysis technique and has proven to be sufficiently accurate. It is considered as one of the most promising approaches in cultural heritage because it is essentially microdestructive and can be used to perform in situ measurements in museums and archaeological sites using portable systems. Figure 1 shows typical LIBS spectra of the microdepth profiling for consecutive pulses on the crust layer compared with spectra of the glaze surface and pottery bulk of shard S1. Comparing the LIBS spectra of glaze, pottery surface, and the in-depth spectra of the black crust shows the appearance and disappearance of the spectral lines of the elements characterizing each layer. For example, in the case of the pottery surface spectrum, the characterizing elements are Fe, Ti, Ca, Mg, and Si. The upper crust layer is very thin about 100  $\mu\text{m}$  and is highly fragile, and the average ablation rate was about 30  $\mu\text{m}$ /pulse. The spectra of black crust obtained by the first laser pulse (30  $\mu\text{m}$  in depth) show the presence of the C(I) line at 247.8 nm, in addition to Fe, Ca, Mg, and Si spectral lines. In all LIBS measurements on the decorating glaze, significant amounts of lead and tin have been observed [16, 18]. Thus, by following up the successive spectra of the upper black layer the intensity of the C(I) line disappears almost completely, while other major spectral lines of glaze start to show up from the second laser pulse after digging about 30  $\mu\text{m}$  in the upper layer. The characteristic glaze lines are Pb(I) at 283.3 nm, and 287.3 nm and Sn, which is hardly detectable after the second pulse, but it has a reasonable intensity after 60  $\mu\text{m}$  in-depth in the third pulse, such as Sn(I) spectral lines at 300.9 nm and 303.4 nm. The source of tin could be due to the presence of mixture of lead-tin yellow ( $\text{Pb}_2\text{SnO}_4$ ) [18]. It is possible to explain the changes in the elemental composition in view of the gradual material removal that takes place in the micro-scale via the laser ablation process. However, the results indicated that there is a noticeable interference between the successive analyzed layers (crust, glazed and pottery layers) especially at the interfaces. Thus, it is even more difficult in the LIBS measurements to distinguish the glaze from pottery contribution on the whole plasma emission because all the major elements of pottery such as Ca, Si, Mg, etc. are also present in the glaze.

Figures 2a, 2b, and 2c show typical zoomed segments of the LIBS spectra of the crust, glaze, and ceramic substrate respectively of shard S2. The lines of C(I) at 247.8 nm and C(II) at 274.7 nm are the most important lines in the crust in addition to lines of iron. The spectrum of the glaze surface of S2 (Fig. 2b) emphasizes the presence of lead and tin as the characterizing elements of the Egyptian glaze. This spectrum shows also the spectral emission lines of Mo, Cr, Si, Mg, and Fe. The presence of Cr and Pb may indicate

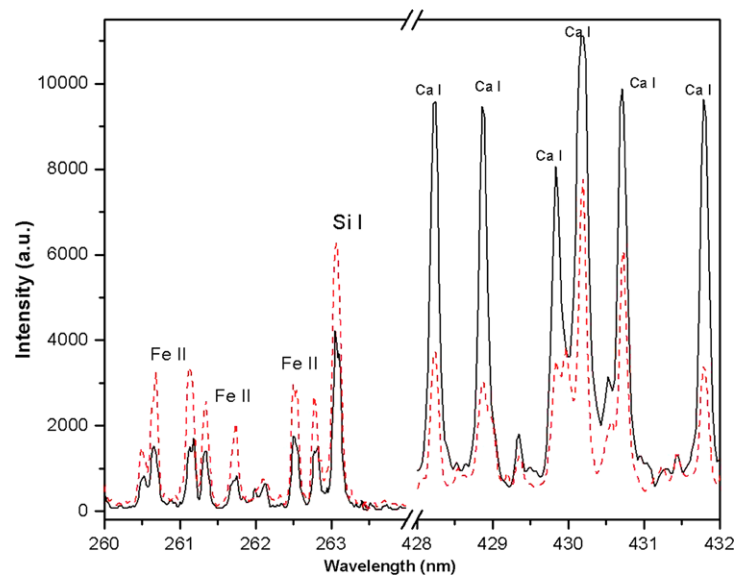
**Fig. 1** Depth profiling of the black crust of shard S1 (corresponding to the ablated thickness for the 1st, 2nd, and 3rd pulses, respectively) that deposited on the glaze surface of 750  $\mu\text{m}$  thickness compared with spectra of the pottery substrate and the glaze surfaces



**Fig. 2** LIBS spectra of (a) the crust 160  $\mu\text{m}$  thick, (b) the glaze 780  $\mu\text{m}$  thick, and (c) the ceramic bulk of the shard S2



**Fig. 3** Comparison between LIBS spectra of the contaminated white crust of 200–500  $\mu\text{m}$  thickness (black-solid) and the substrate of about 8 mm thickness (red-dashed) of sample S3



the use of chrome yellow ( $\text{PbCrO}_4$ ) [28]. The analysis of LIBS spectrum of the white ceramic reveals the characteristic peaks of Ca, Al, and Ti as dominated emissions. The occurrence of Ti can be explained by the use of titanium dioxide as a common component in the ceramics as it grants its white color. In addition, the white ceramic color may be related to the presences of calcium content most likely in the form of calcite ( $\text{CaCO}_3$ ). From this context, the elements spectral lines in a given spectrum can lead to the identification of each compound and the related color on the basis of the detected elements. Consequently, this characterization may lead to the identification of the materials and understanding the technology available to the craftsmen in such ancient eras.

LIBS has been employed also in the elemental analysis of both the upper white crust and the lower ceramic substrate of the shard S3. It was collected from excavation at Sheko Mosque from the Mamluk period. The comparison of LIBS spectra between the upper contaminated crust and pottery depicts the emission lines of Fe that has higher intensity in the spectra of pottery as shown in Fig. 3. In addition, silicon shows up clearly in this part of the pottery spectrum, while calcium lines in the contaminated crust have higher intensity in comparison with that of the bulk pottery. However, a considerable amount of Ca is also found in the bulk pottery as it is considered to be one of the constituents of the clay (Fig. 3).

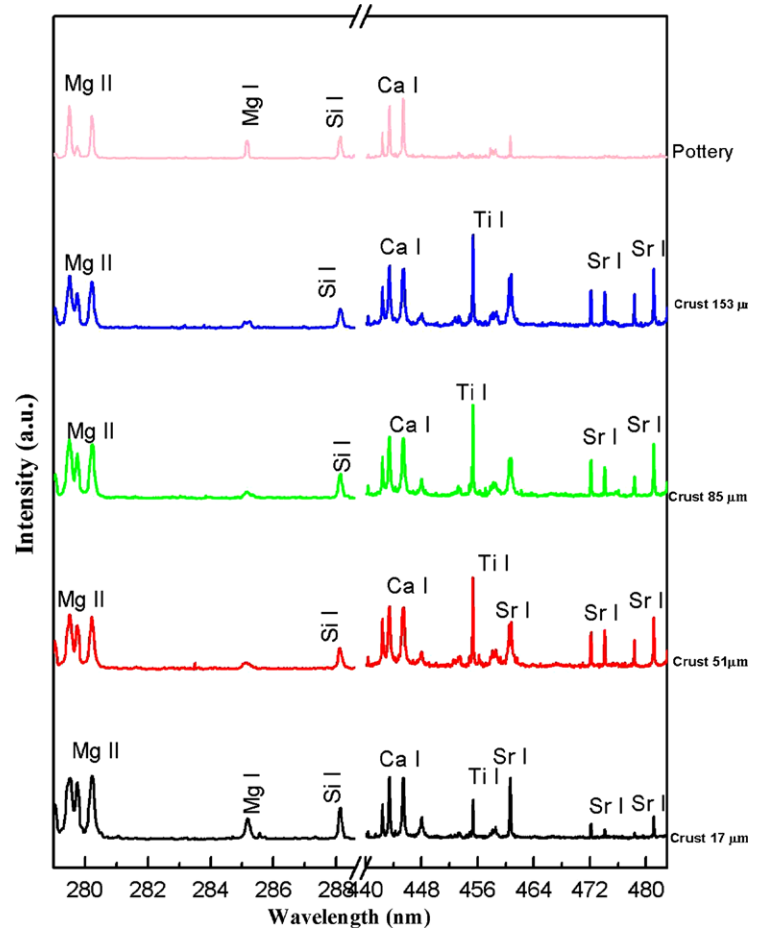
The in-depth analysis of the encrusted shard S4 obtained using the 1st, 3rd, 5th, and 9th laser pulses is shown in Fig. 4. The average mass removal rate (about 17  $\mu\text{m}/\text{pulse}$ ) was from the contaminated crust towards the substrate to provide stratigraphic information about existing elements. It was obvious from the spectra that the spectral lines of elements such as Mg, Ca, and Si show up in both the crust and the

substrate, though their intensities are higher in the spectrum of the upper most layer of the crust. This indicates that these elements are relevant to the surrounding soil that formed the crust. The depth profile of the crust shows clearly the strontium spectral lines (highest in limestone and marl sediments). Such Sr lines are barely detectable in the measured LIBS spectra when we reach in depth the pottery bulk. It is suggested that the enrichment of this element in the crust may be originated due to the presence of celestine ( $\text{SrSO}_4$ ) as proved by XRD results in the next section. Specifically, strontium gives information about carbonate content. It is geochemically associated with calcium and acts as a proxy for calcium in most reactions. One of the primary minerals formed by strontium is strontianite (strontium carbonate), which develops in hydrothermal deposits in limestone and marls. In addition to strontianite, strontium also forms the sulfate mineral Celestine (strontium sulfate), which occurs in limestone and hydrothermal deposits. Additionally, strontium forms in desert lakebeds with gypsum and halite [29].

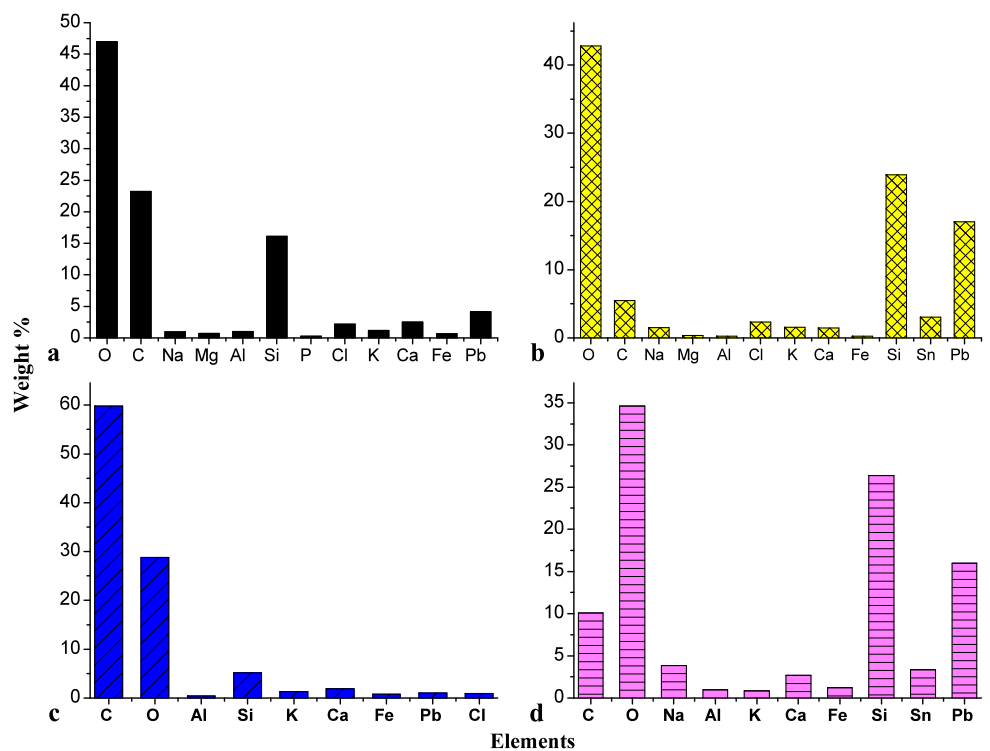
### 3.2 Energy dispersive X-ray (EDX)

Ceramic glazes are a type of anthropogenic glass, and are predominantly made up of silica. As such, it represents a material in which the atoms and molecules are floating around in an unstructured manner. EDX measurements have been performed on the samples S1 and S2 (see Fig. 5) for the upper yellow glazes and their contaminated black layers. The contaminated black thin layer of S1 revealed the presence of metal oxides of Mg, Si, Al, and Ca originating from environmental pollution (Fig. 5a). The black color of the crust seems to be related to the presence of iron that possibly comes from the black mineral of magnetite ( $\text{Fe}_3\text{O}_4$ ), and the presence of carbon. The elements such as Na, Cl, and K have been seen

**Fig. 4** Depth profiling of the black crust of shard S4 (corresponding to the ablated thickness for the 1st, 3rd, 5th, and 9th pulses, respectively) compared with pottery spectra

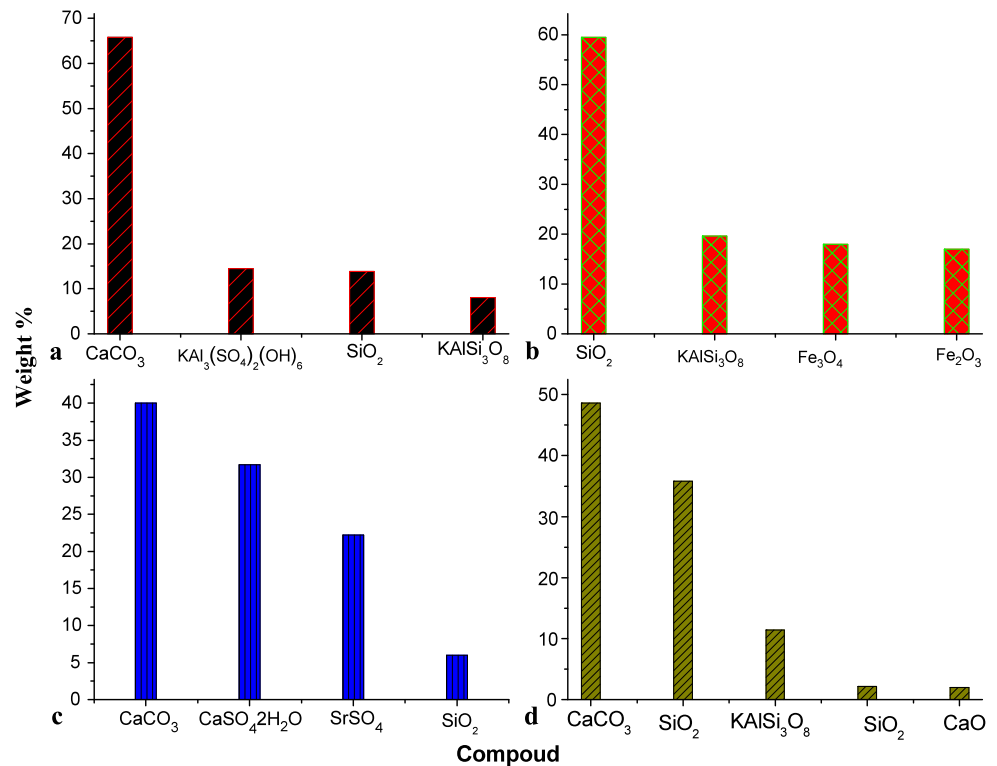


**Fig. 5** Energy dispersive X-ray results for (a) the black layer of shard S1, (b) the glaze layer of S1, (c) the coal layer of S2, and (d) the glaze layer of S2





**Fig. 6** Quantification of the XRD measurements in (a) the contaminated white crust of S3, (b) the pottery surface of S3, (c) the contaminated crust of S4, and (d) the pottery surface of S4



also and could be attributed to the presence of salts in the surrounding soil. The elements (Mg, Na, Al, and Ca) that have been found also in the glazed layer are actually considered part of the formation of glazes. Evidence of Cl, and K were obtained also in both the crust and the glaze as minor elements. Presence of oxygen suggests that most elements are present as oxides. The glaze layer was richer in lead (Pb) than the crust whereas tin (Sn) was detected in the glaze and not in the crust as shown in Fig. 5b. Lead oxide was added as a flux to help in the glaze melting. The glaze main composition is based on the presence of silicon, which exceeds 20 % in wt (Fig. 5b). Alumina was added to stiffen the glaze and prevent it from running off the piece, and tin acts as opacifier. The artificial black coal layer of shard S2 is composed of C, Ca, Fe, O, Si, Pb, Cl, and K as shown in Fig. 5c (the carbon has higher intensity in the LIBS spectra of the crust). For the glaze layer it is composed of lead, tin, and silicon (Fig. 5d).

### 3.3 X-Ray diffraction

Nondestructive X-ray diffraction analysis has been applied on two selected shards, S3 and S4 (the samples were analyzed as it is without powdering them). Standardless quantitative information can be obtained from XRD using Rietveld Analysis [30]. Figure 6 shows the bar graphs of the minerals relative concentration for both the crust and pottery substrate for the two samples. Calcite (CaCO<sub>3</sub>) was the major compound in the contaminated crust of S3

(Fig. 6a); it is composed essentially of pure calcium carbonate derived from limestone, chalk, or marble. Calcite is the most common source of calcium in a glaze and clay body [31]. The majority of calcite in the crust could explain the higher intensity of calcium in the relevant LIBS spectra. The traces in the crust were alunite (KAl<sub>3</sub>(SO<sub>4</sub>)<sub>2</sub>(OH)<sub>6</sub>), quartz (SiO<sub>2</sub>), and orthoclase (KAlSi<sub>3</sub>O<sub>8</sub>). Figure 6b shows the chart of the pottery substrate depicting the presence of quartz (SiO<sub>2</sub>), orthoclase (KAlSi<sub>3</sub>O<sub>8</sub>), magnetite (Fe<sub>3</sub>O<sub>4</sub>), and hematite (Fe<sub>2</sub>O<sub>3</sub>). Iron-rich minerals primarily in the form of hematite upon firing undergo transformation to different dark minerals such as magnetite, and mixed iron oxides (Fe<sub>3</sub>O<sub>4</sub>) [18]. Hematite and magnetite are considered as sources of color in glazes. Hematite converts to magnetite at temperature in the range of 950 to 1250 °C and is often identified in a wide range of artifacts from all over the world because of its long history of use, for instance, in the Egyptian archaeological pottery [29]. XRD analysis of the upper contaminated layer of shard S4 revealed the following minerals: calcite (CaCO<sub>3</sub>), gypsum (CaSO<sub>4</sub>·2H<sub>2</sub>O), celestine (SrSO<sub>4</sub>) and quartz low (SiO<sub>2</sub>) as shown in Fig. 6c. Gypsum originates from the transformation of calcite in the presence of sulfur oxides. It was observed that the encrustation is rich in calcite and gypsum, followed by celestine and relatively poor in quartz. The minerals with higher content in ceramic body were calcite (CaCO<sub>3</sub>) and quartz (SiO<sub>2</sub>) as shown in Fig. 6d. The traces in the ceramic were microcline (KAlSi<sub>3</sub>O<sub>8</sub>), cristobalite low (SiO<sub>2</sub>), and lim (CaO) (Fig. 6d). Quartz and cristobalite are SiO<sub>2</sub> polymorphs, and

the quartz is stable up to 870 °C, then at higher temperature it transforms to cristobalite, however, before this transformation, trimidite could also be formed [9].

#### 4 Conclusion

Laser induced breakdown spectroscopy (LIBS) has been used for in-depth micro-spectrochemical analysis of different encrusted archaeological pottery samples. The aim of this study was to define the constituents of the ceramics to shed light and have better understanding of the exploited technology and available materials for potters in such ancient times. For example, in LIBS spectra results of sample S2, one of the most important constituents in the glaze was lead, and the presence of Cr with Pb may indicate the use of chrome yellow (PbCrO<sub>4</sub>). On the other hand, using the analytical techniques of XRD and EDX lead to additional information in the analysis of ceramics provided by LIBS and there is good agreement in most of the obtained results.

In order to obtain further conclusions about production technologies or provenances, more samples need to be analyzed in future work.

**Acknowledgements** We would like to thank Dr. Hamada Sadek from the Conservation Department, Faculty of Archaeology, Fayoum University, Egypt, for providing some of the ceramic samples.

#### References

1. A. Khedr, V. Papadakis, P. Pouli, D. Anglos, *Appl. Phys. B* **105**(2), 485 (2011)
2. J. Marczak, A. Koss, P. Targowski, M. Góra, M. Strzelec, A. Sarzyński, W. Skrzeczanowski, R. Ostrowski, A. Rycy, *Sensors* **8**, 6507 (2008)
3. G.M. Ingo, E. Angelini, G. Bultrini, T. De Caro, L. Pandolfi, A. Mezzi, *Surf. Interface Anal.* **34**, 328 (2002)
4. G.M. Ingo, E. Angelini, T. de Caro, G. Bultrini, *Appl. Phys. A* **79**, 171 (2004)
5. P. Maravelaki-Kalaitzaki, V. Zafirooulos, C. Fotakis, *Appl. Surf. Sci.* **148**, 92 (1999)
6. G.M. Ingo, E. Angelini, T. de Caro, G. Bultrini, I. Calliari, *Appl. Phys. A, Mater. Sci. Process.* **79**, 199 (2004)
7. J. Pérez-Arategui, A. Larrea, J. Molera, T. Pradell, M. Vendrell-Saz, *Appl. Phys. A* **79**, 235 (2004)
8. P. Mirti, A. Casoli, L. Calzetti, *X-Ray Spectrom.* **25**, 103 (1996)
9. T. Pradell, J. Molera, N. Salvadó, A. Labrador, *Appl. Phys. A* **99**, 407 (2010)
10. R.E. Jones, *Greek and Cypriot pottery, a review of scientific studies. The British School at Athens, Occasional paper* **1**, 1–946 (1986)
11. S. Pagès-Camagna, E. Laval, D. Vigears, A. Duran, *Appl. Phys. A* **100**, 671 (2010)
12. A.G. Karydas, D. Kotzamani, R. Bernard, J.N. Barrandon, C. Zarkadas, *Nucl. Instrum. Methods Phys. Res., Sect. B, Beam Interact. Mater. Atoms* **226**, 15 (2004)
13. N. Mendes, C. Lofrumento, A. Migliori, E.M. Castellucci, *J. Raman Spectrosc.* **39**, 289 (2008)
14. S. Klein, T. Stratoudaki, V. Zafirooulos, J. Hildenhagen, K. Dickmannand, T. Lehmkuhl, *Appl. Phys. A* **69**, 441 (1999)
15. M. Castillejo, M. Martin, D. Silva, T. Stratoudaki, D. Anglos, L. Burgio, R.J.H. Clark, *J. Mol. Struct.* **550–551**, 191 (2000)
16. V. Lazic, F. Colao, R. Fantoni, A. Palucci, V. Spizzichino, I. Borgia, B.G. Brunetti, A. Sgamellotti, *J. Cult. Herit.* **4**, 303 (2003)
17. F.J. Fortes, L.M. Cabalín, J.J. Laserna, *Spectrochim. Acta, Part B, At. Spectrosc.* **63**, 1191 (2008)
18. K. Melessanaki, M. Mateo, S.C. Ferrence, P.P. Betancourt, D. Anglos, *Appl. Surf. Sci.* **197–198**, 156 (2002)
19. M.A. Kasem, R.E. Russo, M.A. Harith, *J. Anal. At. Spectrom.* **26**, 1733–1739 (2011)
20. F.J. Fortes, M. Cortés, M.D. Simón, L.M. Cabalín, J.J. Laserna, *Anal. Chim. Acta* **554**, 136 (2005)
21. O. Abdel-Kareem, M.A. Harith, *Appl. Surf. Sci.* **254**, 5854 (2008)
22. Y. Yoon, T. Kim, M. Yang, K. Lee, G. Lee, *Microchem. J.* **68**, 251 (2001)
23. F. Colao, R. Fantoni, V. Lazic, V. Spizzichino, *Spectrochim. Acta, Part B, At. Spectrosc.* **57**, 1219 (2002)
24. E. Xenogiannopoulou, C. Andreouli, C.J. Stouraras, *J. Nanopart. Res.* **8**, 61 (2009)
25. T. Ctvrtníčková, F.J. Fortes, L.M. Cabalín, V. Kanický, J.J. Laserna, *Surf. Interface Anal.* **41**, 714 (2009)
26. H.-x. Lu, M. He, Y.-y. Liu, J.-f. Guo, L.-w. Zhang, D.-l. Chen, H.-l. Wang, H.-l. Xu, R. Zhang, *J. Ceram Process. Res.* **12**, 588 (2011)
27. <http://rbmason.ca/ceramics.html>
28. C. Fotakis, D. Anglos, V. Zafirooulos, S. Georgiou, V. Tornari, *Lasers in the preservation of cultural heritage, in Principles and Applications*, ed. by R.G.W. Brown, E.R. Pike (Taylor & Francis, New York, 2006)
29. M. Morgenstein, C.A. Redmount, *J. Archaeol. Sci.* **32**, 1613 (2005)
30. H.M. Rietveld, *J. Appl. Crystallogr.* **2**(2), 65–71 (1969)
31. <http://www.sheffield-pottery.com/RAW-MATERIALS-and-CERAMIC-CHEMICALS-s/286.htm>